# Quad-ridge Horn Antenna with Elliptically Shaped Sidewalls

Ockert B. Jacobs, Johann W. Odendaal, *Senior Member, IEEE,* and Johan Joubert, *Senior Member, IEEE*

***Abstract*— A quad-ridge horn antenna is presented as a feed for a reflector antenna for use in radio astronomy applications. The antenna uses elliptically shaped sidewalls to limit the variation of beamwidth over a wide frequency range and to obtain greater radiation pattern rotational symmetry. The antenna is dual-polarized and matched over more than a 4:1 bandwidth. A design procedure is presented and a prototype designed according to this procedure is shown. Measured and simulated results of the prototype correspond well. The antenna is analyzed with a prime focus reflector to determine the range of efficiencies that can be expected.**

***Index Terms*— Radio astronomy, horn antennas, reflector antennas, broadband, antenna feeds.**

## I. Introduction

The square kilometer array [1] is a radio astronomy project that aims at developing and constructing a telescope that is 50 times more sensitive than any current telescope. The SKA aims at achieving this in the high frequency band using approximately 3000 reflector antennas. Existing wide band reflector antenna feeds are incapable of achieving the required sensitivity over the bandwidth of the SKA. New wide band feeds are thus being developed to attain high sensitivity over wide bandwidths [2].

Quad-ridge horn antennas can obtain large bandwidths and are dual polarized [3, 4], however, as an aperture type antenna the expected variation of the beamwidth of a quad-ridge horn is inversely proportional to the aperture size in wavelengths [5, 6]. This makes such antennas less suitable for reflector antenna feeds in cases where high aperture efficiency across the band is required, such as radio astronomy.

Current quad-ridge horn antennas are also typically not adequately matched for radio astronomy applications. This is due to the fact that these antennas are designed for maximum impedance bandwidth [3, 4].

Elliptically shaped waveguide horn antennas and TEM horn antennas have been demonstrated to have beamwidths that vary little with frequency [7, 8]. Waveguide horns, however have limited bandwidth while TEM horns are limited to a single polarization.

Applying elliptically shaped sidewalls to a quad-ridge horn antenna can result in a much larger bandwidth while the radiation pattern is improved by the addition of the shaped sidewalls as has recently been demonstrated [2, 9].

Developing a quad-ridge horn antenna with shaped sidewalls for a smaller bandwidth compared to existing quad-ridge horn antennas could thus result in a feed antenna that is adequately matched, with beamwidths suitable for attaining high aperture efficiency over significantly more than an octave bandwidth (as is typically achieved by corrugated horns).

Another factor that is considered is whether the antenna design can be adapted to achieve a range of -10 dB beamwidths. Designs for new radio astronomy telescopes are investigating the use of different reflector configurations, such as prime focus or offset Gregorian [10, 11]. These require different edge illuminations – having a feed antenna that can be designed to achieve a range of beamwidths would be advantageous.

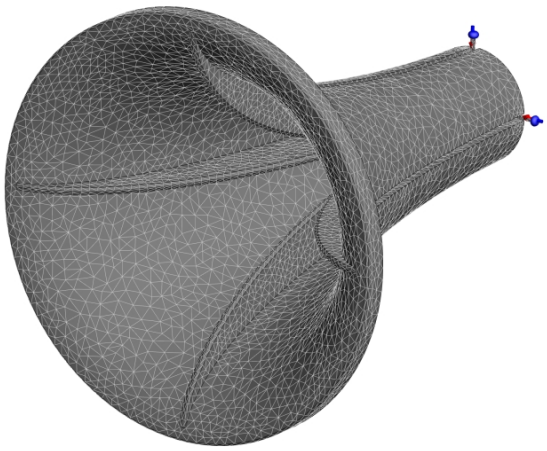

Fig. 1. The geometry of the antenna quad-ridge horn antenna with elliptically shaped sidewall.

This work was supported by the National Research Foundation (NRF) of South Africa.

The authors are with the Centre for Electromagnetism, Department of Electrical, Electronic and Computer Engineering, University of Pretoria, Pretoria, 0002, South Africa (e-mail:s26249822@tuks.co.za).

Measured results are presented that indicate the radiation patterns that were achieved including the cross-polarization in the 45° plane. The phase centre position of the antenna prototype was also evaluated. The aperture efficiency of the feed when used as a prime focus reflector antenna feed was analysed to gain an understanding of the efficiency levels that can be expected when using this antenna. The various efficiency factors when used as a reflector antenna feed, such as spillover, phase, cross-polarization, and taper efficiency, were calculated.

## II. Antenna Modelling

The quad-ridge horn antenna with shaped sidewalls was modeled using FEKO [12] a commercial MoM solver. The antenna was fed using an SMA coaxial connector. The model was fully parametric – allowing changes in the geometry of the model to be easily implemented.

The antenna model included both orthogonal ports, the feed pins needs to cross the gaps between the ridges and as such cannot transition at the same point. The use of symmetry in the solution was thus not possible. The transition from SMA connector to an airline was also included – although the characteristic impedance of the two lines are the same the change in the physical size of the coaxial connectors could result in deteriorated VSWR due to the physical discontinuity, this step (the inner and outer conductor is stepped smaller) can be seen in Fig. 2. The dielectric of the SMA connector was modeled using the surface equivalence principle.

The ridges and the back cavity as well as the flared section of the ridges were optimized to provide a good match to a 50 Ω coaxial line. Such low impedance could only be achieved by using a waveguide that has a small gap between opposing ridges. The small ridge gap was realized by using chamfered ridges. The feed area is shown in Fig. 2. The closely spaced ridges allowed the antenna to be well matched to the 50 Ω line over a wide bandwidth.

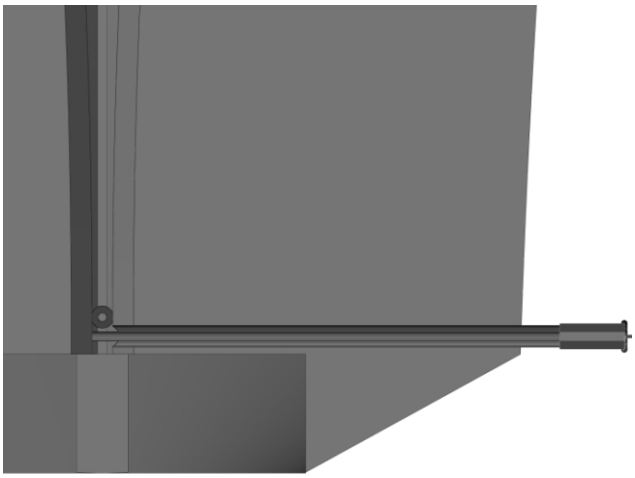

Fig. 2 Side view with a cut plane of the feed area of the antenna.

## III. Parametric Study

The parametric model of the quad-ridge antenna was used to conduct a parametric study to determine how different parameters affect the performance of the antenna. The antenna can be broadly divided into two sections, the waveguide transition, a transition from coaxial line to quad-ridge waveguide that included parameters such as the quad-ridge waveguide size, shape, ridge thickness, ridge gap and distance to the backshort and the horn flared section that includes the ridge profile and the sidewall parameters.

As expected, waveguide parameters have little effect on the radiation patterns. The exception to this was that the backshort and waveguide parameters controlled higher order mode propagation. These areas thus had to be designed with care so that wide bandwidth can be obtained. The impedance characteristics were also determined to a large extent by this section of the antenna.

Parameters in the flare section mainly determined the radiation characteristics of the antenna. The most effective control over the beamwidth could be obtained by manipulating the profile of the elliptically shaped horn section. The elliptical shape of the antenna was modified by changing the ratio between the length of the horn and the width of the aperture as demonstrated in Fig 3.

Other parameters also affected the beamwidth but the control over beamwidth was limited and changes to these parameters, such as the ridge profile, tended to also strongly affect the impedance matching.

The parametric study also indicated how to design the waveguide section, the ridge width, gap between the ridges and waveguide diameter, of the antenna to obtain good impedance matching.

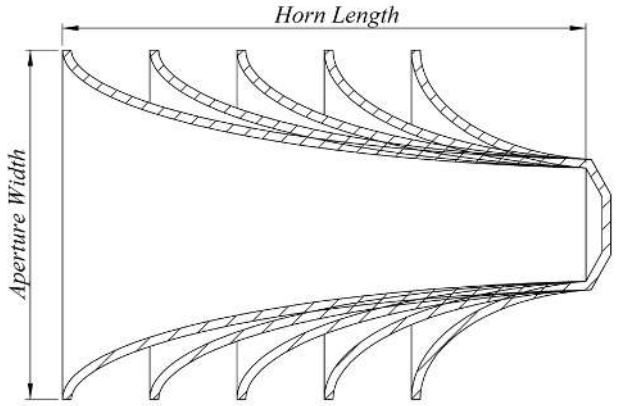


Fig. 3. Quad-ridge horn antennas with different ratios of horn length to aperture diameter.

Another factor that was considered is how well the antenna can be designed to achieve a specific beamwidth. Table 1

demonstrates that a wide range of reasonably constant beamwidths could be achieved for different ratios between the aperture diameter and the horn length for elliptically shaped quad-ridge horn antennas. Quad-ridge horn antennas that are well matched and have 10 dB beamwidths of between 60 and 90 degrees could be obtained using this method. It can be seen in Table 1 that the ratio has a large effect on the average beamwidths and that certain combinations of ratio and aperture size resulted in E- and H-plane beamwidths that are closer together.

TABLE I
THE MEAN 10 DB BEAMWIDTH (IN DEGREES) FROM 1 TO 3 GHZ

| Model | Plane | R = 0.5 | R = 0.75 | R = 1.0 | R = 1.25 | R = 1.5 |
|---|---|---|---|---|---|---|
| AP = 350 | E | 107.15 | 89.13 | 76.84 | 69.46 | 64.13 |
| | H | 97.20 | 90.27 | 86.15 | 82.37 | 78.81 |
| AP = 400 | E | 105.77 | 87.69 | 74.69 | 65.66 | 59.88 |
| | H | 92.15 | 85.79 | 80.90 | 76.92 | 73.06 |
| AP = 450 | E | 106.21 | 85.65 | 73.01 | 63.20 | 56.90 |
| | H | 88.16 | 81.59 | 76.68 | 72.24 | 68.32 |
| AP = 500 | E | 105.43 | 84.47 | 71.19 | 61.71 | 54.89 |
| | H | 84.97 | 78.06 | 73.04 | 68.56 | 64.43 |

## IV. Antenna Design and Manufacturing

The results of the parametric study were used to design a prototype antenna. The prototype was designed for a shaped sub-reflector antenna that required a feed taper of 17 dB at 50 degrees. The approximate elliptical profile ratio required for this beamwidth level was obtained from the parametric study. This ratio was then fine-tuned to obtain the required beamwidth. The size of the aperture is then adapted to reduce the variation in beamwidth level and obtain patterns that are more rotationally symmetrical.

The design of the prototype antenna is shown in Fig. 1 and 4. The antenna has a maximum diameter of 480 mm with a total length of 585 mm. The large size is due to the high gain (narrow beamwidth) that is required and the low frequency.

The sidewall was machined in a number of inter-locking aluminium sections. The sections slotted together and were held in position by the four ridges. Each section bolted to the ridges and due to the curvature of the sidewall and ridges the sections were held tightly in position. The ridges also slotted and bolted into the conical backshort to ensure symmetry at the feed point of the antenna.

The outer profile of the antenna was designed to improve manufacturability, only the first stepped section was modeled as this had the greatest effect on the radiation pattern – beyond this the outer profile had very little effect. The gaps between sections were also modeled to ensure that manufacturing the sidewall in sections did not impact on the performance of the prototype. It was found that gaps of up to 0.5 mm have little effect on the antenna performance. An exploded view of the assembly of the antenna is shown in Fig. 4, indicating how the various parts are assembled.

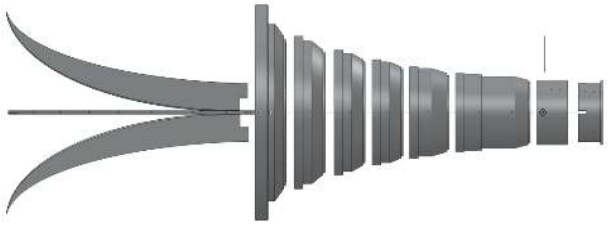

Fig. 4. An exploded view of the antenna indicating part assembly.

## V. Results

The antenna Voltage Standing Wave Ratio (VSWR) and coupling were measured using an HP 8510 vector network analyser. The antenna aperture was pointed at a sheet of radar absorbent material during measurement. The measured VSWR of the antenna is compared to simulated results in Fig. 5.

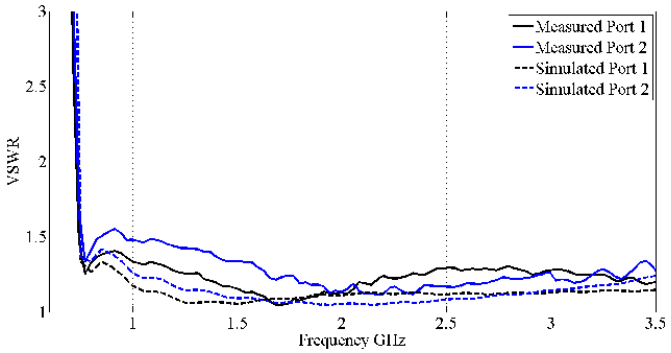


Fig. 5. Comparison of the measured and simulated VSWR.

The measured and simulated results agree reasonably well. The measured results did not quite achieve the low predicted reflection coefficient, but followed the same trend as the simulated results. The reflection coefficient of port 1 was better than 1.5:1 for the 4:1 band while port 2 had a maximum value of just more than 1.5:1 in this band with values significantly below 1.5:1 dB for a large portion of the band. The antenna is also well matched over more than a 4:1 band (0.75 to 3GHz).

The VSWR measurements showed that the feed region of the antenna – the transition from SMA to air-line dielectric, and the connection of the feed pin to the connector strongly influenced the measurements. Obtaining good positive contact between the feed pin and the connector receptacle was essential to achieving good return loss across the band. Good

contact between the sidewall and the connector outer was also required to ensure good return loss. The antenna feed section thus has to be assembled with great care. The measured and simulated coupling between orthogonal ports is shown in Fig. 6. The measured coupling between ports was better than 30 dB.

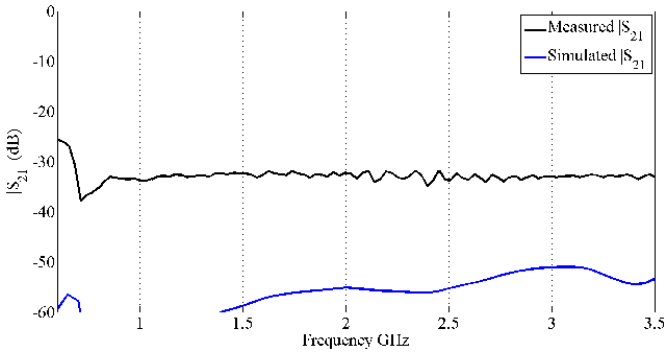


Fig. 6. The measured and simulated coupling between orthogonal ports.

The measured boresight gain of the antenna is compared to the simulated gain in Fig. 7. The measured and simulated gain show good agreement with less than 1 dB deviation from the predicted level up to 3 GHz.

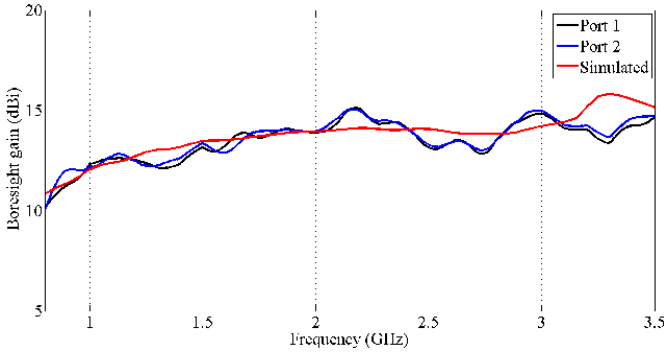


Fig. 7. Comparison between measured and simulated boresight gain.

The measured and simulated 10 dB beamwidths are compared in Fig. 8. The measured and simulated results show excellent agreement the largest error being smaller than 6°. The beamwidth is reasonably constant across the band of interest and the principal plane beamwidth are also close (with a maximum difference of 14° up to 3 GHz) indicating a reasonably rotationally symmetrical radiation pattern. The radiation patterns are shown on the following two pages for a number of frequencies. As the radiation patterns of the two ports closely matched each other the results are shown only for port 1. The principle plane patterns and 45° degree plane co- and cross polarization is shown.

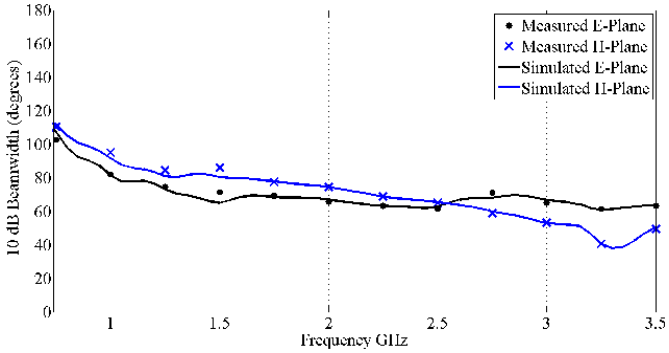


Fig. 8. Comparison between measured and simulated 10 dB beamwidth.

The cross polarization is shown only in the 45° degree plane as it tends to be a maximum there. The measured and simulated radiation patterns of the antenna are shown in Fig. 9 and 10 from 0.75 to 3 GHz.

## VI. Reflector Antenna Analysis

As a reflector feed the antenna has to be capable of using the available surface of the reflector with high efficiency while limiting radiation past the dish edge, which is especially undesirable in radio astronomy as it causes an increase in noise temperature.

The efficiency of the antenna when used as a reflector feed was estimated using a prime focus reflector antenna configuration. The reflector aperture efficiency is calculated using two methods. The simulated radiation patterns are integrated to calculate the efficiencies and the reflector antenna is analyzed using hybrid Method of Moments – Physical Optics (MoM-PO), in FEKO, with the aperture efficiency of the reflector being calculated from the gain. Coupling between the MoM and PO solutions was not implemented and both calculation methods thus did not take into account aperture blockage. Pattern integration allows the aperture efficiency to be separated into a number of efficiency factors that are detailed below [13].

- Spill-over efficiency. The power lost due to the part of the feed antenna radiation pattern that does not illuminate the reflector.
- Taper efficiency. The deviation of the feed antenna radiation pattern from a uniform amplitude distribution. Parts of the reflector that are not fully illuminated are under-utilised and cause the efficiency to drop.
- Phase efficiency. The deviation of the feed antenna radiation pattern from an equiphase distribution and defocusing loss due to phase centre variation.
- Cross-polarization efficiency. The power lost due to unwanted cross-polarization incident on the reflector aperture.

The good agreement that was obtained between measured and simulated patterns allowed the simulated radiation patterns to be used to calculate these efficiency factors.

Simulated results for a full pattern solid angle can be obtained easily using computational electromagnetics and as measured and simulated efficiencies (on the principal plane) have shown good agreement, can be used to accurately estimate efficiency factors for radiation patterns that are not strictly rotationally symmetric. The cross-polarization of the horn also has strong variations as a function of the azimuth angle which can easily be taking into account by using the full, simulated pattern – ensuring that cross-polarization efficiency is inaccurately estimated.

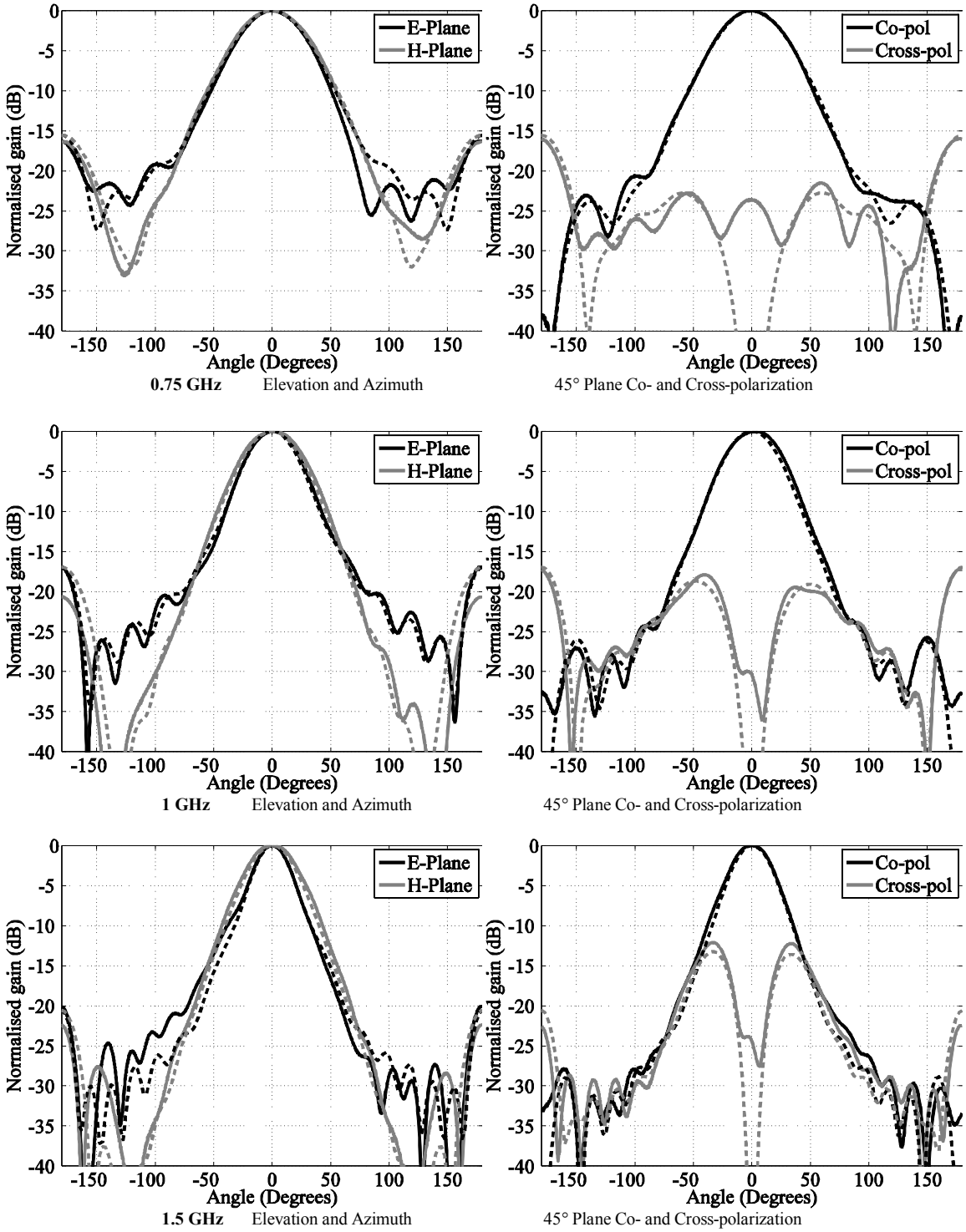


Fig. 9. Radiation patterns of the quad-ridge horn antenna up to 1.5 GHz (Measured: Solid and simulated: Dashed).

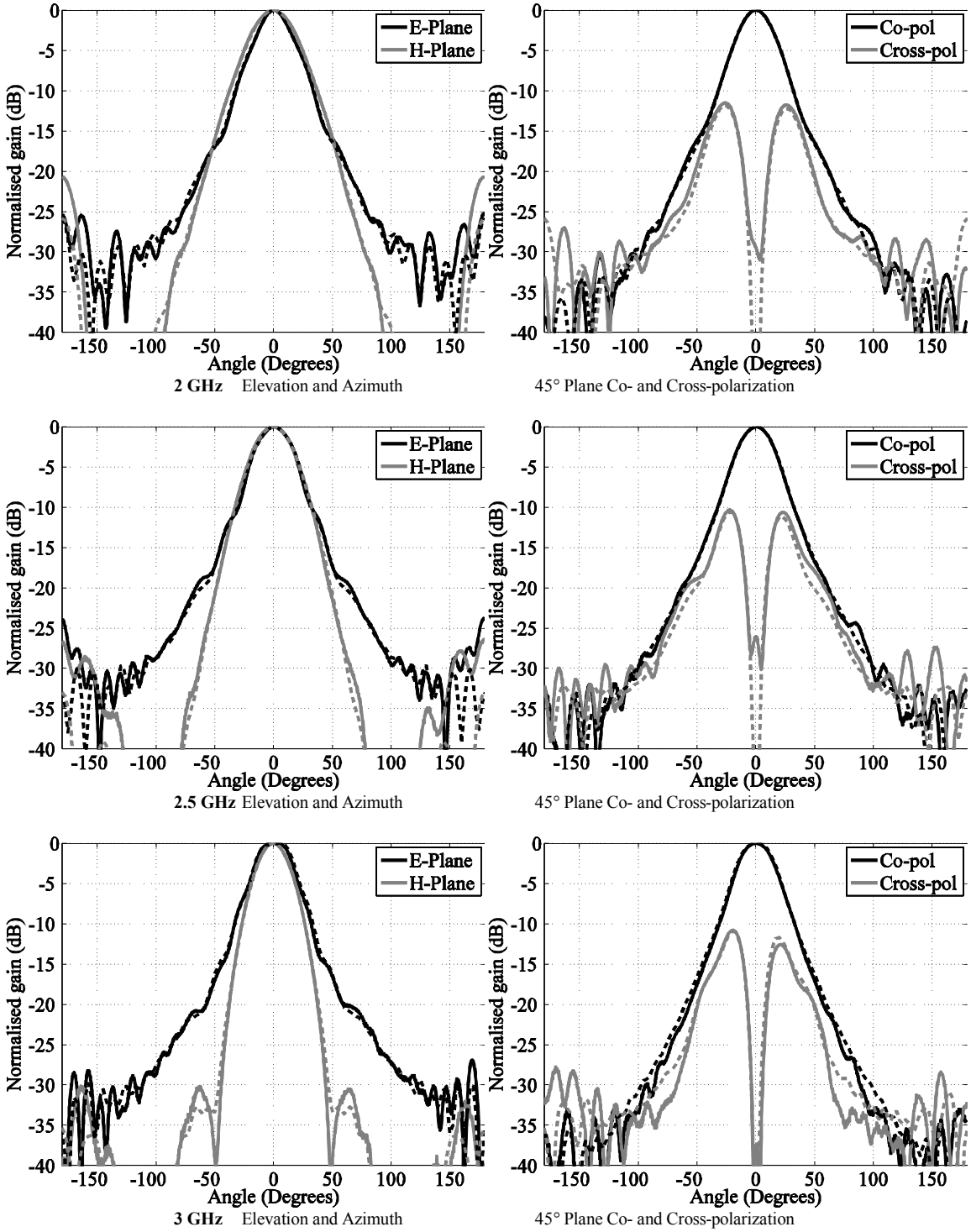


Fig. 10. Radiation patterns of the quad-ridge horn antenna up to 3 GHz (Measured: Solid and simulated: Dashed).

A prime focus reflector antenna with a half angle of 35° was found to give reasonably high efficiency over the band of interest. This half angle corresponds to an *F/D* ratio of 0.793. A 12 m diameter reflector antenna would thus have a focal point located at 9.515 m from the reflector. The large *F/D* ratio was required for high efficiency as the feed antenna has a very narrow beamwidth. Such a large *F/D* ratio might require a different reflector configuration to realize physically (with an effective focal length), for example a Cassegrain configuration. The prime focus reflector antenna configuration is shown in Fig. 11.

The antenna was positioned by calculating the phase reference position that resulted in the highest average phase efficiency across the band, using simulated patterns.

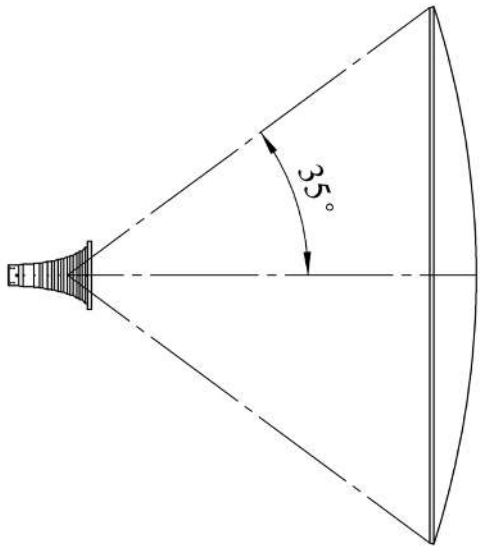


Fig. 11. The reflector antenna configuration.

The antenna was then position so that this phase reference position coincided with the focal point of the reflector. The taper efficiency of the antenna positioned in such a way was calculated both for simulated and measured results. The comparison is shown in Fig. 12.

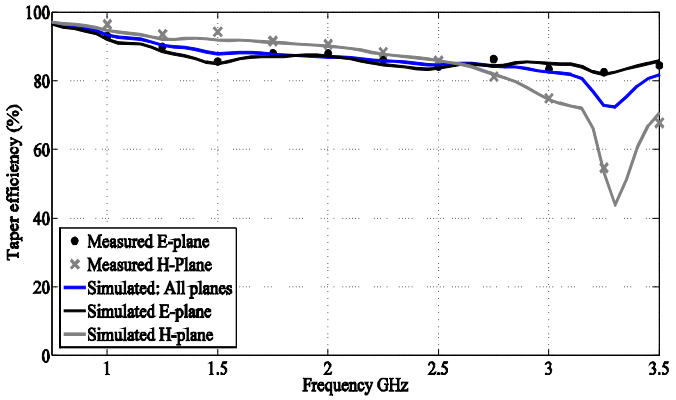


Fig. 12. Comparison of the measured and simulated taper efficiencies in the principal planes.

It can be seen that the results agree very well, also shown is the result obtained when using the simulated pattern over a full solid angle.

The efficiency factors of the antenna when used as a feed for the 35° prime focus parabolic reflector antenna is shown in Fig. 13. All four the efficiency factors as well as their product, the aperture efficiency is shown. The efficiency factors calculated from the simulated patterns are also compared to the aperture efficiency calculated using a hybrid method of moments (MoM) – physical optics (PO) approach to validate the calculation. This approach consists of solving the horn section of the problem using MoM and using these results to calculate the radiation patterns of the reflector-horn combination using PO. The MoM and PO solutions were decoupled.

The aperture efficiency was calculated from the maximum directivity obtained by simulating the feed and reflector antenna combination. It is seen that the aperture efficiencies obtained agrees very well with one another.

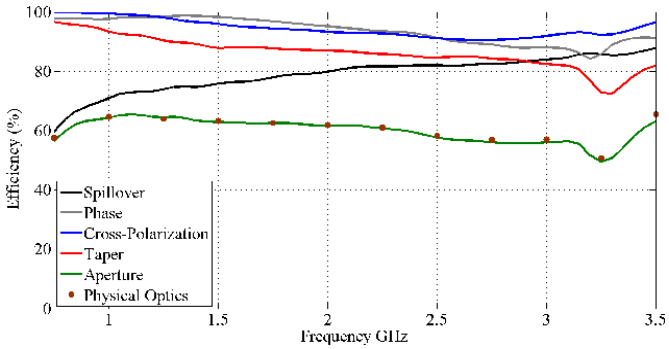


Fig. 13. Efficiencies of the quad-ridge horn antenna in a 12 m 35° prime focus parabolic reflector antenna compared to a physical optics approximation.

The antenna obtains reasonably high aperture efficiency up to approximately 3.5 GHz (larger than 50%) with the efficiency being more than 60% over a large part of the band. Beyond 3.5 GHz the efficiency drops off.

## VII. Conclusion

Radio astronomy reflector antennas require feeds that can give high efficiency and low spill-over over a broad bandwidth. This requires radiation patterns with a constant beamwidth and a sharp cut-off beyond the reflector edge. A quad-ridge horn antenna with elliptically shaped sidewalls was developed that proved capable of achieving these requirements reasonably successfully.

The quad-ridge horn antenna was modelled using Method of Moments. The antenna model was used to conduct a parametric study that identified parameters of the quad-ridge horn antenna that affected the radiation pattern and how these parameters could be manipulated to obtain radiation patterns more suited for radio astronomy reflector antenna feeds. A prototype antenna was designed using the results of the parametric study.

The performance of the prototype quad-ridge horn antenna with elliptically shaped sidewalls has been presented. Good agreement between measured and simulated results was obtained for the prototype. The antenna was well matched over a relative bandwidth larger than 4:1 (0.75 GHz to 3 GHz). Good radiation patterns that were reasonably constant and rotationally symmetrical were obtained. Analysis of the antenna with a reflector antenna, using both pattern integration with 3D simulated patterns and Physical Optics (PO) indicated that the antenna would be capable of achieving high aperture efficiencies (larger than 55 %) over at least a 4:1 bandwidth.

## REFERENCES


[1] SKA. (2010, March). The Square Kilometer Array: The International Radio Telescope for the 21st Century. [Online]. Available: http://www.skatelescope.org /PDF/brochure/ SKA_Brochure_2009.pdf

[2] *O*.B. Jacobs, J.W. Odendaal and J. Joubert, "Elliptically shaped quad-ridge horn antennas as feed for a reflector," *Antennas Wireless Propag. Lett.*, vol. 10, pp. 756 – 659, Jul. 2011.

[3] V. Rodriguez, "A multi-octave, open-boundary, quad-ridge horn antenna for use in the S- to Ku-bands," *Microwave Journal*, vol. 49, no. 3, Mar. 2006.

[4] Z. Shen and C. Feng, "A new dual-polarized broadband horn antenna," IEEE Antennas Wireless Propag. Lett., vol. 4, pp. 270-273, 2005.

[5] M. Gilbert, K. Higgins, and L. Romero, "Quad-ridge Horn Utilizing Resistive Films to Reduce Sidelobes", IEEE Antennas and Propagation Society Int. Symp., 2007. pp. 5684-5687, 9-15 June 2007.

[6] C.F. Parker and R.J. Anderson, "Constant Beamwidth Broadband Antennas," *IRE International Convention Record*, 1957, vol. 5, pp. 87-98.

[7] J.A.G Malherbe and Y. Katcondia, "An elliptically flared waveguide horn," *Microwave and Optical Technology Letters*, vol. 52, no. 9, Sept. 2010.

[8] J.A.G Malherbe, "Frequency-independent performance of elliptic profile TEM horns," Microwave and optical technology letters, vol. 51, no. 3, pp. 607 – 612, Mar. 2009.

[9] *W.A. Imbriale and A. Akgiray, "*Performance of a quad-ridged feed in a wideband Radio Telescope," *Proceedings of the 5th European Conference on Antennas and Propagation*, 2011, pp. 662 – 665.

[10] C.A. Balanis, *Antenna Theory Analysis and Design*, 3rd ed., Hoboken, NJ: Wiley, 2005.

[11] W.L. Stutzman and G.A. Thiele, Antenna Theory and Design, 2nd ed., Hoboken, NJ: Wiley, 1998.

[12] FEKO User's Manual Suite 6.0, EM Software & Systems – S.A. (Pty) Ltd, Stellenbosch, South Africa, Sept. 2010.

[13] IEEE Standard Definitions of Terms for Antennas, IEEE Std 145-1993, 18 March 1993.